



Prediction of HCC microvascular invasion with gadobenate-enhanced MRI: correlation with pathology

Ling Zhang¹ · Xian Yu² · WenXin Wei³ · XingPeng Pan⁴ · Lun Lu⁴ · JinJu Xia⁴ · Wei Zheng⁴ · Ningyang Jia⁴ · Lei Huo⁴

Received: 9 June 2019 / Revised: 4 March 2020 / Accepted: 14 April 2020 / Published online: 4 May 2020
© European Society of Radiology 2020

Abstract

Purpose To assess the accuracy of gadobenate-enhanced MRI for predicting microvascular invasion (MVI) in patients operated for hepatocellular carcinoma (HCC).

Methods The 164 patients who met the inclusion criteria were assigned to one of two groups: the MVI-positive group and the MVI-negative group. Imaging results were compared between the two groups using the Kruskal test, chi-square test, independent sample *t* test, and logistic regression analysis.

Results Differences in the capsule ($p = 0.037$) and margin ($p = 0.004$) of the tumor, rim enhancement ($p = 0.002$), peritumoral enhancement in the arterial phase ($p < 0.001$), and peritumoral hypointensity in the hepatobiliary phase (HBP) ($p < 0.001$) were statistically significant. The results of multivariate analysis identified rim enhancement in the arterial phase (odds ratio (OR) = 2.115; 95% confidence interval (CI), 1.002–4.464; $p = 0.049$) and peritumoral hypointensity in the HBP (OR = 5.836; 95% CI, 2.442–13.948; $p < 0.001$) as independent risk factors for MVI. Use of the two predictors in combination identified 32.79% (20/61) of HCCs with MVI with a specificity of 95.15% (98/103).

Conclusions Rim enhancement in the arterial phase and peritumoral hypointensity in the HBP were identified as independent risk factors for MVI in patients with HCC.

Key Points

- Rim enhancement in the arterial phase and peritumoral hypointensity in the hepatobiliary phase were independent risk factors for microvascular invasion in patients with HCC.
- Use of the two predictors in combination had a sensitivity of 32.79% and a specificity of 95.15% for predicting microvascular invasion.

Keywords Hepatocellular carcinoma · Liver neoplasms · Risk factors · Magnetic resonance imaging · Gadolinium

Abbreviations

ADC	Apparent diffusion coefficient
AFP	Alpha-fetoprotein
DCE	Dynamic contrast-enhanced
Gd-BOPTA	Gadobenate dimeglumine
HBP	Hepatobiliary phase

HCC	Hepatocellular carcinoma
MVI	Microvascular invasion
PIVKA-II	Protein Induced by Vitamin K Absence or Antagonist-II
SI	Signal intensity

Ling Zhang and Xian Yu contributed equally to this work.

✉ Ningyang Jia
jianingyang6@163.com

✉ Lei Huo
leidfgd@163.com

¹ Department of Radiology, Nanfang Hospital, Southern Medical University, Guangzhou 510515, China

² Department of Gastrointestinal Surgery, Chongqing University Cancer Hospital & Chongqing Cancer Institute & Chongqing Cancer Hospital, Chongqing 400030, China

³ Department of Hepatic Surgery, Eastern Hepatobiliary Surgery Hospital, Second Military Medical University, Shanghai 200438, China

⁴ Department of Radiology, Eastern Hepatobiliary Surgery Hospital, Second Military Medical University, Shanghai 200438, China

Introduction

Microvascular invasion (MVI) is an important predictor of hepatocellular carcinoma (HCC) recurrence after surgical resection or liver transplantation, particularly recurrence during the early period [1–5]. Predicting MVI using preoperative imaging indicators would be of great clinical significance. Recent studies reported that certain imaging manifestations may help the preoperative diagnosis of MVI, including size, capsule, margin, signal intensity (SI) ratio of the tumor, apparent diffusion coefficient (ADC) values, peritumoral enhancement and rim enhancement in the arterial phase, and peritumoral hypointensity of the tumor in the hepatobiliary phase (HBP) of gadoxetate disodium-enhanced MRI [6–14]. An et al reported that both rim enhancement and peritumoral enhancement in the arterial phase are independent risk factors for MVI and HCC recurrence [7]. Lee et al [9] demonstrated that arterial peritumoral enhancement, non-smooth tumor margin, and peritumoral hypointensity on gadoxetic acid-enhanced HBP images were independent and significant predictors of MVI in HCC. However, there is no clinical consensus regarding the optimal imaging parameter for predicting MVI accurately.

Gadobenate dimeglumine (Gd-BOPTA) is a biphasic T1-weighted MRI contrast agent characterized by nonspecific distribution in the extracellular space and specific uptake in hepatocytes. This agent can be used not only for dynamic contrast-enhanced (DCE) MRI of the liver but also for specific imaging in the HBP within 40 to 120 min after being injected. However, no research on predicting MVI using Gd-BOPTA-enhanced MR imaging manifestations has been reported.

Here, we evaluated the diagnostic efficacy of Gd-BOPTA-enhanced MRI imaging signs for predicting MVI in patients operated for HCC.

Materials and methods

Patients

A retrospective study was performed including 463 patients who underwent MRI scan in Shanghai Eastern Hepatobiliary Hospital between September 2016 and June 2017.

The inclusion criteria were as follows: (1) 18–80 years old; (2) liver tumors of more than 1 cm in diameter as determined by MR images; (3) Gd-BOPTA-enhanced MRI scan including complete arterial phase, portal phase, delayed phase, and HBP examination recording; (4) surgical removal of the tumor; and (5) HCC diagnosed by postoperative pathology (Fig. 1).

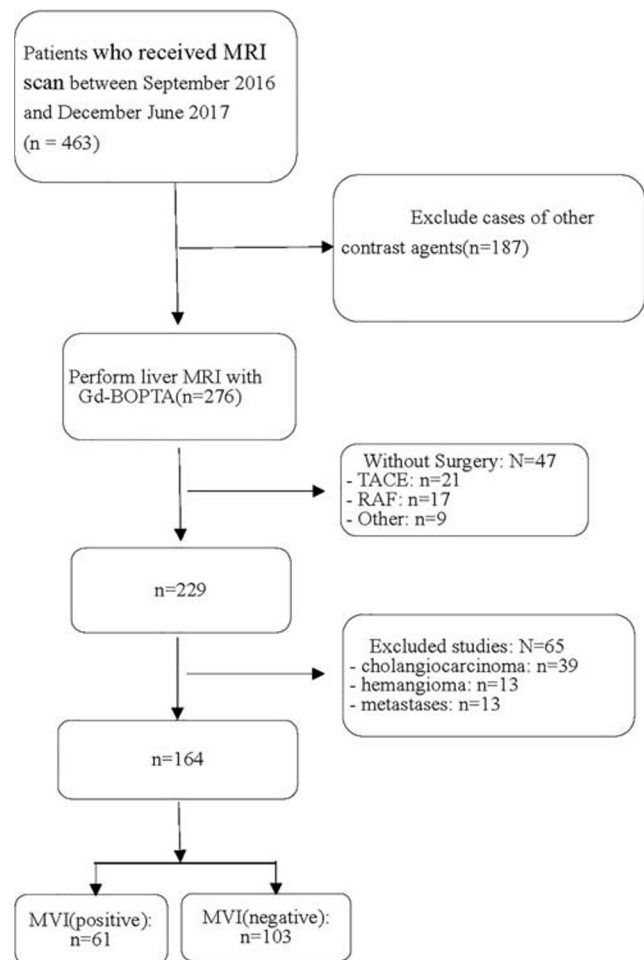


Fig. 1 Flow chart of the study population. HCC: hepatocellular carcinoma; TACE: transcatheter arterial chemoembolization

MRI scan

MRI was performed with the GE Optima MR360 1.5 T with an 8-channel abdominal coil. All patients fasted for 4 h before the scan. Gd-BOPTA (MultiHance, Bracco) at 0.1 mmol/kg was injected into patients' median cubital veins at a flow rate of 2.0 mL/s with a high-pressure syringe. The enhanced scan of the arterial, portal, and delayed phases was performed at 22–25 s, 50–60 s, and 90–120 s after the injection of Gd-BOPTA, respectively. Scanning at the HBP in patients with normal liver function and those with impaired function was performed at 60 min and 120 min after the injection of the contrast agent, respectively. The definition of impaired liver function was performed based on the clinical assessment by the referring physicians.

Table 1 summarizes the scanners and scanning parameters. FIESTA, T1WI (in-phase/opposed-phase), and fat-suppressed T2-weighted images were acquired. Dynamic contrast-enhanced MRI was performed using Gd-BOPTA, and the 3D-LAVA (Liver Acquisition with Volume Acceleration) technique was used.

Table 1 Sequences and parameters of Gd-BOPTA dynamic-enhanced MRI

Sequences	Image plane	TR/TE (msec)	FOV (mm)	Flip angle	Thickness (mm)	Matrix	Scanning order
FIESTA	C	3.5/1.5	420 × 420	60	6	160 × 224	1
T1WI (in-phase/opposed-phase)	A	190/4.3(2)	420 × 420	80	6	256 × 160	3
T2WI	A	6667/85	420 × 420	160	6	320 × 224	4
LAVA	A	3.7/1.7	420 × 420	15	2.5	256 × 192	5
2D MRCP	Oblique	4000/847	320 × 320	160	50	320 × 256	6
HBP	A	3.7/1.7	420 × 420	15	2.5	256 × 192	7
HBP	C	3.7/1.7	400 × 400	15	2.5	256 × 192	8

A axial; C coronal

Clinical and imaging data analysis

Clinical data were obtained from the electronic patients' records. The MR imaging manifestations were analyzed by two radiologists, both with more than 10 years of experience in abdominal imaging, working in consensus. The clinical parameters assessed included patient gender, age, protein induced by vitamin K absence/antagonist-II (PIVKA-II), alpha-fetoprotein (AFP), HBsAg, HBeAg, and cirrhosis. Imaging parameters included intratumoral fat, rim and peritumoral enhancement in the arterial phase, hypointensity, and peritumoral hypointensity in the HBP.

The Liver Imaging Reporting and Data System (2017) (LI-RADS-2017) was used as the reference standard for assessments of tumor size, capsule, and margins [15]. The size of a tumor was determined across the longest diameter of the largest plane of the mass including the capsule. Tumor margins were defined as smooth or non-smooth, with the latter demonstrating peritumoral buds on transverse and coronal HBP images [8]. The presence of intratumoral fat was defined as a fat fraction (FF) of > 5%, which was calculated using the following formula: $FF = (\text{in-phase} - \text{opposed-phase})/2 \times \text{in-phase}$ [16]. The capsule refers to the smooth peripheral hyperenhancement in the portal venous or delayed phases [17]. Peritumoral enhancement in the arterial phase was defined as a crescent or polygonal enhanced region outside the margin of the tumor showing extensive contact with the margin and similar signal intensity to that of the normal liver parenchyma in the delayed phase [18]. Peritumoral hypointensity in the HBP refers to a wedge-shaped or flame-like hypointensity area outside the margin compared with that of the normal liver parenchyma [11].

Pathological analysis

All tumor sections were reexamined by an experienced pathologist with 21 years of experience in pathological diagnosis of liver cancers. The WHO Classification of Tumors of the Digestive System (2010) [19] defines MVI as the presence of

cancer cell nests in the vascular lumen lined by endothelial cells under the microscope, which is dominated by branches of portal veins (including blood vessels inside the capsule). The cases were divided into MVI-positive and MVI-negative groups. Cirrhosis of the liver was diagnosed by the pathologist during the histopathological examination of hepatocellular carcinoma.

Statistical analysis

Categorical data were analyzed using the chi-square test or Fisher's exact test, and continuous variables were analyzed using analysis of variance or the Kruskal-Wallis *H* test for variables with an abnormal distribution and homogeneity of variance. Univariate logistic regression was used to identify independent predictors of MVI. Variables identified as significant in the univariate analysis were included in the multivariate analysis model. After considering the effect of capsule, arterial rim enhancement, arterial peritumoral enhancement, tumor margin, peritumoral hypointensity in the HBP, and shape, the adjusted odds ratio (OR), and 95% confidence interval (CI) were estimated. All statistical tests were two-sided, and *p* values of < 0.05 were considered statistically significant. Data compilations and descriptive statistics were performed using SPSS 19.0 for Windows (IBM).

Results

Clinical data and laboratory examination

Overall, 164 patients met the inclusion criteria. The median interval between MRI examination and surgery was 9 days for all patients, and the longest interval was 16 days.

There were 125 patients in the normal liver function group and 39 patients in the impaired liver function group. The average age was 55.9 ± 10.31 years, and the male-to-female ratio was 139:25 (Table 2). There were 61 patients

Table 2 Comparison of patient characteristics according to microvascular invasion

Characteristics	Total	MVI = 0 (negative)	MVI = 1 (positive)	<i>p</i>
Sex	164	103	61	0.559
Male	139	86	53	
Female	25	17	8	
Age	55.90 (10.31)	55.38 (10.43)	56.77 (10.12)	0.405
Size (cm)				0.385
< 5	58	39	19	
≥ 5	106	64	42	
PIVKA-II	133.50 (34.75, 744.50)	133.50 (30.50, 744.50)	149.50 (38.50, 833.25)	0.449
AFP (ng/L)				0.167
> 0, ≤ 20	72	51	21	
> 20, ≤ 400	58	33	25	
> 400	29	16	13	
HBsAg				0.300
Negative	28	20	8	
Positive	136	83	53	
HBeAg				0.648
Negative	119	76	43	
Positive	45	27	18	
Cirrhosis				0.618
Negative	44	29	15	
Positive	120	74	46	
MRI features				
Radiological capsule				<i>0.037</i>
Negative	122	71	51	
Positive	42	32	10	
Lipid				0.166
Negative	113	67	46	
Positive	51	36	15	
Arterial rim enhancement				<i>0.002</i>
Negative	87	64	23	
Positive	77	39	38	
Arterial peritumoral enhancement				<i>< 0.001</i>
Negative	145	98	47	
Positive	19	5	14	
Tumor margin				<i>0.004</i>
Smooth	78	58	20	
Non-smooth	86	45	41	
Tumor hypointensity on HBP				0.647
Yes	150	95	55	
No	14	8	6	
Peritumoral hypointensity on HBP				<i>< 0.001</i>
Absent	123	92	31	
Present	41	11	30	
Shape				0.964
Round	46	29	17	
Oval	23	14	9	
Lobular	60	39	21	
Irregular	35	21	14	

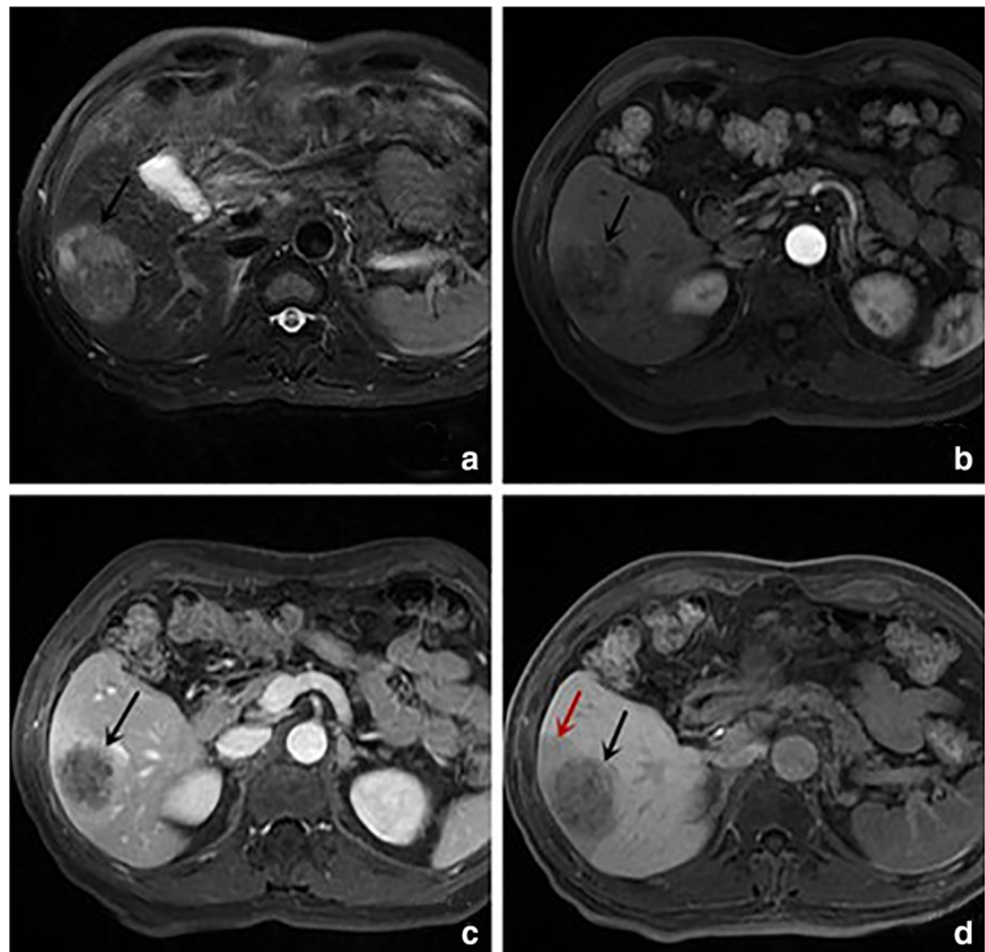
The italicized entries signify *p* values < 0.05

in the MVI-positive group and 103 in the MVI-negative group. In the MVI-positive group, the male-to-female ratio was 53:8, and the average age was 56.77 ± 10.12 years; in the MVI-negative group, the ratio was 86:17, and the average age was 55.38 ± 10.43 years. There were no statistically significant differences in the average age, male-to-female ratio, size and number of tumors, liver nodules, cirrhosis, and the levels of AFP and PIVKA-II in the serum between the two groups ($p > 0.05$).

Gd-BOPTA-enhanced MR imaging manifestations

The differences in the shape of tumors and intratumoral fat between the two groups were not statistically significant ($p = 0.166$). There were statistically significant differences between the MVI-positive group and MVI-negative group in the capsule (16% vs. 31%, respectively, $p = 0.037$) and non-smooth margin (67% vs. 44%, respectively, $p = 0.004$) (Figs. 2 and 3) of tumors, rim enhancement (62% vs. 38%,

Fig. 2 HCC presenting with MVI in a 59-year-old man. **a** Unevenly high signals on T2WI; **b, c** Slight heterogeneous enhancement (black arrow) on the arterial phase with washout and non-smooth margin on the delayed phase. **d** Non-smooth tumor margin and peritumoral hypointensity (red arrow) in the hepatobiliary phase



respectively, $p = 0.002$; Fig. 4), and peritumoral enhancement (23% vs. 5%, respectively, $p < 0.001$) (Figs. 2 and 3, red arrow) in the arterial phase. In the HBP, there was a statistically significant difference in peritumoral hypointensity between the MVI-positive group and MVI-negative group (48% vs. 10%, respectively, $p < 0.001$), whereas the difference in intratumoral hypointensity in the HBP was not statistically significant (90% vs. 92%, respectively, $p = 0.647$).

Multivariate analysis identified rim enhancement in the arterial phase (OR = 2.115; 95% CI, 1.002–4.464; $p = 0.049$) and peritumoral hypointensity in the HBP (OR = 5.836; 95% CI, 2.442–13.948; $p = 0.001$) as independent risk factors for MVI (Table 3).

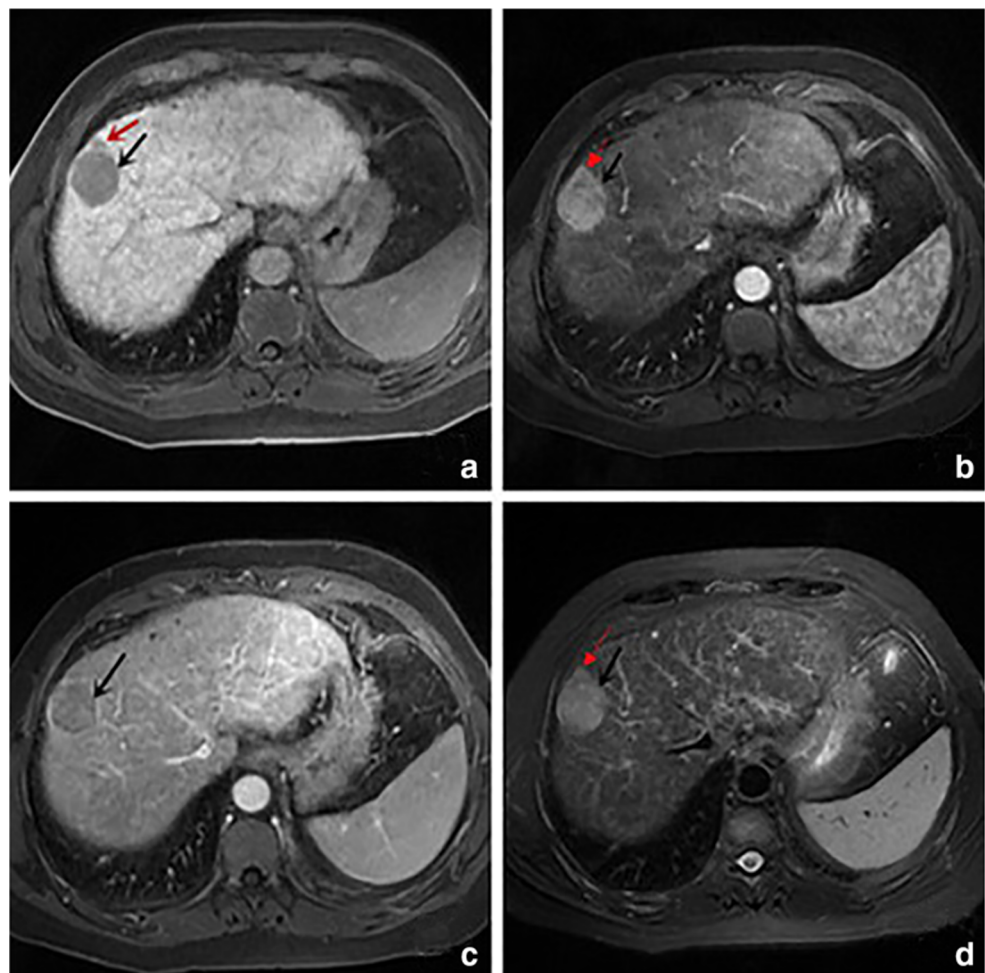
The results of logistic regression analysis indicated that two imaging features could help predict MVI: the rim enhancement of the tumor in the arterial phase and peritumoral hypointensity in the HBP. The sensitivity, specificity, accuracy, PPV, and NPV of each feature and their combination for predicting MVI are listed in Table 4. When the two features were used simultaneously, they were combined in two ways as follows: either feature was positive for MVI (parallel connection) or both features were positive for MVI (serial connection). The parallel connection identified 78.69% (48/61) of

HCCs with MVI with a specificity of 56.31%. The serial connection method identified 32.79% (20/61) of HCCs with MVI with a specificity of 95.15%. As shown in Table 4, the serial connection method had a higher specificity and PPV than the parallel connection method.

Discussion

The present study showed that rim enhancement in the arterial phase and peritumoral hypointensity in the HBP were independent risk factors for MVI in patients with HCC. MVI is an important factor in predicting the recurrence of HCC after surgical resection. Patient gender, age, tumor size, the levels of serum PIVKA-II and AFP, hepatitis B infection, and cirrhosis did not differ significantly between the MVI-positive and MVI-negative groups in our study. Biochemical indicators, diseases associated with HCC, and tumor size were not useful for predicting MVI before surgery. Large tumor size generally indicates that MVI is more likely to occur in HCC. However, the usefulness of tumor size alone for predicting MVI in HCC is controversial [6], and these conflicting results could be attributed to selection bias. In the present cohort,

Fig. 3 HCC with MVI in a 48-year-old man. **a** The lesion is moderately hyperintense and well-delineated in the liver parenchyma on T2WI. **b, c** It shows clear homogeneous arterial phase hyperenhancement with washout on the delayed phase and enhancing capsule. **d** On the HBP image, the lesion is hypointense and well-delineated in liver parenchyma, and shows a peripheral tumor node



tumor lesions larger than 5 cm accounted for 64% (106/164). Future studies should include a larger number of patients with tumors of different sizes, which may increase the value of tumor size for predicting MVI.

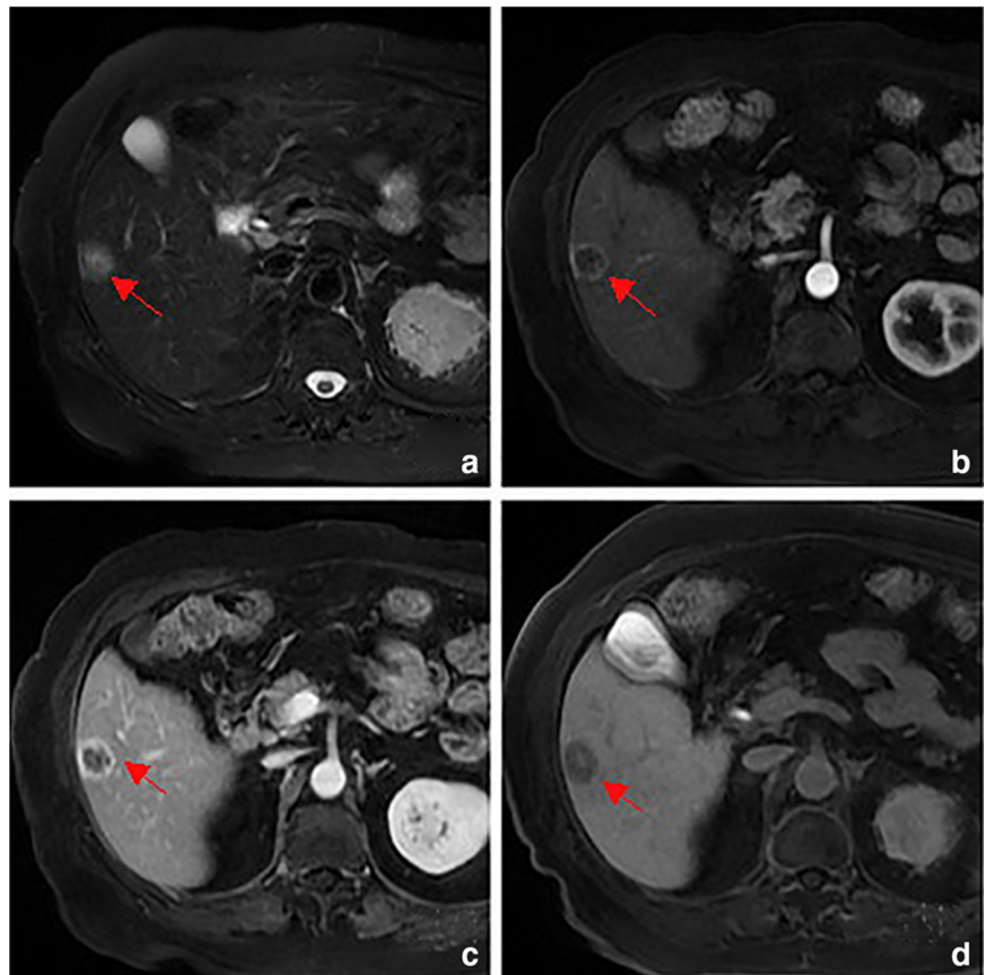
Several studies have investigated ways to predict MVI using MR imaging manifestations, such as the diameter and margins of the lesion, enhancing mode, and DWI signals before surgical resection of HCC. The use of gadoxetic acid disodium, a hepatocyte-specific contrast agent, in the clinical setting led to studies investigating the effect of MR imaging manifestations (such as signal intensity and peritumoral hypointensity in the HBP) to try to predict the occurrence of MVI before surgical resection of HCC [6–10].

The HCC capsule as an imaging manifestation refers to the proliferating fibrous connective tissues encircling the tumor, which are caused by the growth of the tumor. The capsule is actually a “pseudo-capsule” because it does not contain epithelial tissues. One study [20] reported that the presence of a capsule in live tumors is an indicator of a poor prognosis, whereas another report [21] indicated that the fibrous “pseudo-capsule” may help limit the growth of cancers, thereby predicting a good prognosis. Our data indicated that capsules

are more likely to occur in MVI-negative patients. The difference in the presence of a capsule was statistically significant between the two groups ($p = 0.037$). The results of univariate analysis demonstrated that the absence of a capsule is a risk factor for MVI ($p = 0.040$). However, the results of multivariate analysis showed that it was not an independent risk factor ($p = 0.550$), namely, the absence of a capsule was not an indicator of the occurrence of MVI.

Previous studies [22–26] reported that the occurrence of MVI can be predicted by assessing the characteristics of the margin and that a non-smooth margin is an independent risk factor for MVI. In the present study, the results of univariate analysis indicated that a non-smooth margin is an indicator of MVI, whereas multivariate analysis showed that it is not an independent risk factor for MVI, which was similar to a previous report [27]. We classified tumors into round, oval, lobular, and irregular to explore the association between the shape of tumors and MVI. The results showed no statistically significant differences in the shape of tumors between the two groups ($p = 0.964$). The effect of tumor shape on predicting MVI needs to be further evaluated in future studies.

Fig. 4 HCC with MVI in a 55-year-old man. **a** T2WI showed a moderately hyperintense lesion with smooth margin. **b, c** The lesion was rim enhancement during the arterial phase and delayed phase (red arrow). **d** On the HBP image, the lesion is hypointense



In the present study, there was no statistically significant difference in the lipid ratio between the two groups ($p = 0.166$). We speculate that MVI may be caused by insufficient

peripheral arterial blood supply resulting from damaged peritumoral hepatocytes (as indicated by peritumoral hypointensity in the HBP) and obstructed drainage veins.

Table 3 Univariate and multivariate analyses of preoperative MR imaging findings in predicting microvascular invasion

	Univariate analysis		Multivariate analyses	
	OR (95% CI)	<i>p</i>	OR (95% CI)	<i>p</i>
Capsule	0.435 (0.196, 0.964)	<i>0.040</i>	0.754 (0.298, 1.908)	0.550
Lipid	1.648 (0.810, 3.350)	0.168	1.592 (0.724, 3.501)	0.248
Rim enhancement	2.711 (1.411, 5.210)	<i>0.003</i>	2.115 (1.002, 4.464)	<i>0.049</i>
Arterial peritumoral enhancement	5.838 (1.985, 17.170)	<i>0.001</i>	1.767 (0.518, 6.031)	0.363
Tumor margin	2.642 (1.364, 5.119)	<i>0.004</i>	1.823 (0.850, 3.910)	0.123
Tumor hypointensity on HBP	1.295 (0.427, 3.928)	0.647		
Peritumoral hypointensity on HBP	8.094 (3.630, 18.046)	<i>< 0.001</i>	5.836 (2.442, 13.948)	<i>< 0.001</i>
Shape		0.964		
Round	0.879 (0.356, 2.170)	0.780		
Oval	0.964 (0.329, 2.829)	0.947		
Lobular	0.808 (0.342, 1.908)	0.626		

The italicized entries signify p values < 0.05

Table 4 Diagnostic performance of MR imaging findings in prediction of microvascular invasion

	Sensitivity	Specificity	Accuracy	PPV	NPV
Rim enhancement	62.30 (38/61)	62.14 (64/103)	62.20 (102/164)	49.35 (38/77)	73.56 (64/87)
Peritumoral hypointensity on HBP	49.18 (30/61)	89.32 (92/103)	74.39 (122/164)	73.17 (30/41)	74.80 (92/123)
Parallel connection*	78.69 (48/61)	56.31 (58/103)	51.61 (106/164)	51.61 (48/93)	81.69 (58/71)
Series connection [#]	32.79 (20/61)	95.15 (98/103)	71.95 (118/164)	80.00 (20/25)	70.50 (98/139)

The italicized entries signify p values < 0.05

*Either method result is positive for positive microvascular invasion

[#] Both method results are positive for positive microvascular invasion

Rim enhancement of a tumor in the arterial phase indicated invasive growth in the absence of the capsule, the occurrence of MVI, and rapid growth with central necrosis. Peritumoral enhancement in the arterial phase indicated enhancement of the normal peritumoral hepatic parenchyma. This was caused by hemodynamic changes of the surrounding hepatic parenchyma, decreased blood supply in the portal vein, and increased blood supply in the arteries when the small peritumoral blood vessels are invaded by HCC. In the present study, the incidence of rim enhancement and peritumoral enhancement in the arterial phase was higher in the MVI-positive group than that in the MVI-negative group, and the difference was statistically significant ($p = 0.002$; $p < 0.001$). The results of univariate analysis identified the two predictors as risk factors for MVI ($p = 0.003$; $p = 0.001$); however, multivariate analysis indicated that rim enhancement, but not peritumoral enhancement, is an independent risk factor for MVI, which is not consistent with the findings of previous studies. Several studies have shown that peritumoral enhancement in the arterial phase is associated with MVI [18, 28]. An et al demonstrated that both rim enhancement and peritumoral enhancement in the arterial phase are independent risk factors for MVI and HCC recurrence [7]. Lee et al reported that peritumoral enhancement in the arterial phase is an independent risk factor for MVI, whereas rim enhancement is not [9]. These discrepancies could be attributed to sample bias or differences in sample size. Future studies should include additional cases with Gd-BOPTA-enhanced MRI data to clarify which clinical and imaging indicators are stable and reliable independent predictors of MVI.

Manifestations on the HBP images of Gd-BOPTA-enhanced MRI reflect the function of hepatocytes. HCC cells, which originate from hepatocytes, cannot absorb Gd-BOPTA in the HBP. This causes intratumoral hypointensity in this phase. In this study, the difference in the occurrence of intratumoral hypointensity in the HBP between the two groups was not statistically significant (55/61 vs. 95/103; $p = 0.647$), whereas the difference in the incidence of peritumoral hypointensity in the HBP was statistically significant ($p < 0.001$). Peritumoral

hypointensity in the HBP suggested that the liver cells around the tumor were damaged and their metabolic function was impaired. Peritumoral hypointensity was more frequent in the MVI-positive group. The results of univariate and multivariate analyses showed that peritumoral hypointensity in the HBP was an independent risk factor for MVI, which is consistent with previous reports [9, 10].

Combined with the findings of previous studies, the present results indicated that rim enhancement in the arterial phase and peritumoral hypointensity in the HBP were independent risk factors for MVI in patients with HCC. Simultaneous use of the two features identified 32.79% (20/61) of HCCs with MVI with a specificity of 95.15% (98/103).

The present study had several limitations. Firstly, patients with multicentric (or very large) tumors who are not surgical candidates could not be included in the study, which may decrease the value of certain risk factors for predicting the incidence of MVI. This could explain the relatively low incidence of MVI in the present series. Secondly, we did not compare the two groups in terms of ADC values because of retrospective design; we failed to enforce the scanning of DWI data from all the patients with sufficient quality, in which 13 patients did not have DWI imaging during initial scan protocol for reasons like motion artifacts from inadequate breathholding. In addition, the relatively high incidence of rim enhancement in the arterial phase (77/164) in this study may have led to false ADC values. Moreover, the determination of accurate ADC values may be affected by the large average tumor size (40 mm), large areas of necrosis, cystic degeneration, and hemorrhage in the central areas of the large tumors with relatively small areas of intratumor parenchymal tissue. Relatively few patients can accurately measure ADC values and may introduce a selection bias. Finally, another limitation of the study was the lack of inter-observer evaluation. The original aim of this study was to verify that MVI has certain imaging signs; therefore, discrepancies between the observers' first impressions were not recorded. The agreement between observers needs to be tested in future studies.

A larger sample and follow-up are needed to reduce the bias caused by the low rate of MVI-positive cases and to verify the association between the imaging manifestations and HCC prognosis and recurrence.

Conclusion

Rim enhancement in the arterial phase and peritumoral hypointensity in the HBP were identified as independent risk factors for MVI. When the two factors were used in combination, the specificity of MVI prediction in HCC reached 95.15%.

Acknowledgments We would like to thank the whole study team at 4 hospitals, for continuous support.

Funding information This study has received funding from the Natural Science Foundation of Guangdong Province (2018A030313951), the Foundation of President of Nanfang Hospital (2017C011), the National Science and Technology Major Project (2018ZX10302207-004), the China Medical Research Fund of Guangdong Province (A2017496).

Compliance with ethical standards

Guarantor The scientific guarantor of this publication is Chenguang Wang.

Conflict of interest The authors of this manuscript declare no relationships with any companies, whose products or services may be related to the subject matter of the article.

Statistics and biometry Professor Cairong Zhu kindly provided statistical advice for this manuscript.

Informed consent Written informed consent was not required for this study because Gd-BOPTA had been widely used in MRI scan as a contrast agent.

Ethical approval Institutional Review Board approval was obtained.

Methodology

- retrospective
- diagnostic study
- performed at one institution

References

- Banerjee S, Wang DS, Kim HJ et al (2015) A computed tomography radiogenomic biomarker predicts microvascular invasion and clinical outcomes in hepatocellular carcinoma. *Hepatology* 62:792–800
- Lee S, Kim KW, Jeong WK et al (2019) Gadoteric acid-enhanced MRI as a predictor of recurrence of HCC after liver transplantation. *Eur Radiol* 30:987–995
- Wei Y, Huang ZX, Tang HH et al (2019) IVIM improves preoperative assessment of microvascular invasion in HCC. *Eur Radiol* 29:5403–5414
- Feng ST, Jia YM, Liao B et al (2019) Preoperative prediction of microvascular invasion in hepatocellular cancer: a radiomics model using Gd-EOB-DTPA-enhanced MRI. *Eur Radiol* 29:4648–4659
- Ahn SY, Lee JM, Joo I et al (2015) Prediction of microvascular invasion of hepatocellular carcinoma using gadoteric acid-enhanced MR and (18) FFDG PET/CT. *Abdom Imaging* 40:843–851
- Renzulli M, Brocchi S, Cucchetti A et al (2016) Can current preoperative imaging be used to detect microvascular invasion of hepatocellular carcinoma? *Radiology* 279:432–442
- An C, Kim DW, Park YN, Chung YE, Rhee H, Kim MJ (2015) Single hepatocellular carcinoma: preoperative MR imaging to predict early recurrence after curative resection. *Radiology* 276:433–443
- Ariizumi S, Kitagawa K, Kotera Y et al (2011) A non-smooth tumor margin in the hepatobiliary phase of gadoteric acid disodium (Gd-EOB-DTPA)-enhanced magnetic resonance imaging predicts microscopic portal vein invasion, intrahepatic metastasis, and early recurrence after hepatectomy in patients with hepatocellular carcinoma. *J Hepatobiliary Pancreat Sci* 18:575–585
- Lee S, Kim SH, Lee JE (2017) Preoperative gadoteric acid-enhanced MRI for predicting microvascular invasion in patients with single hepatocellular carcinoma. *J Hepatol* 67:526–534
- Kim JY, Kim MJ, Kim KA, Jeong HT, Park YN (2012) Hyperintense HCC on hepatobiliary phase images of gadoteric acid-enhanced MRI: correlation with clinical and pathological features. *Eur J Radiol* 81:3877–3882
- Kim KA, Kim MJ, Jeon HM et al (2012) Prediction of microvascular invasion of hepatocellular carcinoma: usefulness of peritumoral hypointensity seen on gadoteric acid disodium-enhanced hepatobiliary phase images. *J Magn Reson Imaging* 35:629–634
- Suh YJ, Kim MJ, Choi JY, Park MS, Kim KW (2012) Preoperative prediction of the microvascular invasion of hepatocellular carcinoma with diffusion-weighted imaging. *Liver Transpl* 18:1171–1178
- Xu P, Zeng M, Liu K, Shan Y, Xu C, Lin J (2014) Microvascular invasion in small hepatocellular carcinoma: is it predictable with preoperative diffusion-weighted imaging? *J Gastroenterol Hepatol* 29:330–336
- Okamura S, Sumie S, Tonan T et al (2016) Diffusion weighted magnetic resonance imaging predicts malignant potential in small hepatocellular carcinoma. *Dig Liver Dis* 48:945–952
- Elasys KM, Hooker JC, Agrons MM et al (2017) Version of LI-RADS for CT and MR imaging: an update. *Radiographics*. 37: 1994–2017
- Reeder SB, Sirlin CB (2010) Quantification of liver fat with magnetic resonance imaging. *Magn Reson Imaging Clin N Am* 18:337–357
- Choi JY, Lee JM, Sirlin CB (2014) CT and MR imaging diagnosis and staging of hepatocellular carcinoma: part II. Extracellular agents, hepatobiliary agents, and ancillary imaging features. *Radiology* 273:30–50
- Kim H, Park MS, Choi JY et al (2009) Can microvessel invasion of hepatocellular carcinoma be predicted by pre-operative MRI? *Eur Radiol* 19:1744–1751
- Bosman F, Carneiro F, Hruban R (2010) WHO classification tumours of the digestive system. IARC Press, Lyon
- Zhang J, Liu XJ, Zhang HP et al (2019) Texture analysis based on preoperative magnetic resonance imaging (MRI) and conventional MRI features for predicting the early recurrence of single hepatocellular carcinoma after hepatectomy. *Acad Radiol* 26:1164–1173
- Ng IO, Lai EC, Ng MM, Fan ST (1992) Tumor encapsulation in hepatocellular carcinoma. A pathologic study of 189 cases. *Cancer* 70:45–49

22. Nakashima Y, Nakashima O, Tanaka M, Okuda K, Nakashima M, Kojiro M (2003) Portal vein invasion and intrahepatic micrometastasis in small hepatocellular carcinoma by gross type. *Hepatol Res* 26:142–147
23. Eguchi S, Takatsuki M, Hidaka M et al (2010) Predictor for histological microvascular invasion of hepatocellular carcinoma: a lesson from 229 consecutive cases of curative liver resection. *World J Surg* 34:1034–1038
24. Nagano Y, Shimada H, Takeda K et al (2008) Predictive factors of microvascular invasion in patients with hepatocellular carcinoma larger than 5 cm. *World J Surg* 32:2218–2222
25. Chou CT, Chen RC, Lee CW et al (2012) Prediction of microvascular invasion of hepatocellular carcinoma by preoperative CT imaging. *Br J Radiol* 85:778–783
26. Wu TH, Hatano E, Yamanaka K et al (2016) A non-smooth tumor margin on preoperative imaging predicts microvascular invasion of hepatocellular carcinoma. *Surg Today* 46:1275–1281
27. Hu HT, Wang Z, Huang XW et al (2018) Ultrasound-based radiomics score: a potential biomarker for the prediction of microvascular invasion in hepatocellular carcinoma. *Eur Radiol* 29:2890–2901
28. Miyata R, Tanimoto A, Wakabayashi G et al (2006) Accuracy of preoperative prediction of microinvasion of portal vein in hepatocellular carcinoma using superparamagnetic iron oxide-enhanced magnetic resonance imaging and computed tomography during hepatic angiography. *J Gastroenterol* 41:987–995

Publisher's note Springer Nature remains neutral with regard to jurisdictional claims in published maps and institutional affiliations.